Journal of Physics D: Applied Physics

Properties of dielectric barrier discharges in extended coplanar electrode systems

To cite this article: Valentin I Gibalov and Gerhard J Pietsch 2004 *J. Phys. D: Appl. Phys.* **37** 2093

View the article online for updates and enhancements.

Related content

- Dielectric barrier discharges in coplanar arrangements
  Valentin I Gibalov and Gerhard J Pietsch
- Development of dielectric barrier discharges
  Valentin I Gibalov and Gerhard J Pietsch
- Dynamics of dielectric barrier discharges in different arrangements
  Valentin I Gibalov and Gerhard J Pietsch

Recent citations

- How do the barrier thickness and dielectric material influence the filamentary mode and CO_2 conversion in a flowing DBD?
  A Ozkan *et al*
- Dielectric barrier discharges revisited: the case for mobile surface charge
  F J J Peeters *et al*
- Marcel Šimor and Yves Creyghton

IOP ebooks™

Bringing you innovative digital publishing with leading voices to create your essential collection of books in STEM research.

Start exploring the collection - download the first chapter of every title for free.

This content was downloaded from IP address 203.246.85.161 on 30/01/2019 at 07:17

INSTITUTE OF PHYSICS PUBLISHING JOURNAL OF PHYSICS D: APPLIED PHYSICS

J. Phys. D: Appl. Phys. **37** (2004) 2093–2100 PII: S0022-3727(04)81785-6

Properties of dielectric barrier discharges in extended coplanar electrode systems

Valentin I Gibalov[1] **and Gerhard J Pietsch**[2]

[1] Department of Chemistry, Moscow State University, Leninsky gory, 119899 Moscow, Russia
[2] Gas Discharge Engineering, RWTH Aachen University, Schinkelstr. 2, 52056 Aachen, Germany

E-mail: pietsch@ifht.rwth-aachen.de and gibalov@valentin.chem.msu.su

Received 9 June 2004
Published 14 July 2004
Online at stacks.iop.org/JPhysD/37/2093
doi:10.1088/0022-3727/37/15/007

Abstract
Barrier discharges in coplanar arrangements consists of a multitude of discharge channels (microdischarges) on the dielectric surface. The parameters of such an ensemble of channels are investigated numerically using a two-dimensional model. The channel width and density along extended pairs of electrodes are introduced in the model in order to obtain a more accurate description of the behaviour of the whole device. Using this model voltage–charge curves (Lissajous figures) can be calculated. The simulated voltage–charge curves, the device capacitances for the conditions discharge 'on' and 'off', inception voltages and current densities are obtained. They correspond well with experimental results.

(Some figures in this article are in colour only in the electronic version)

1. Introduction

Coplanar discharge (CD) arrangements are characterized by pairs of electrodes incorporated in the bulk of a dielectric near a surface [1]. Breakdown occurs in the gas medium on the dielectric surface in the form of thin channels, which originate and terminate at the locations of the electrodes on the dielectric surface (figure 1).

The filament structure is common for barrier discharges in gas gaps and on surfaces (e.g. [2]). The average distance between the channels is of the order of the inter-electrode gap. The channels seem to appear simultaneously and develop rather independent of their neighbours. The preceding channels influence the succeeding ones through surface charges left on the dielectric surface. The behaviour of an individual channel has been investigated in another paper in detail [1].

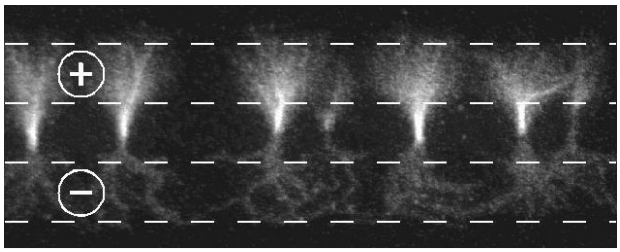

Figure 1. CCD picture of a CD in atmospheric air. The location of the electrodes is marked with dotted lines, the inter-electrode distance is 2 mm and the exposure time half a cycle of the applied voltage [3].

The aim of this paper is to obtain parameters (to describe the properties) of entire CD devices, i.e. of an arrangement with extended electrodes where numerous discharge channels determine the properties of the CD. The parameters of such a device have been determined experimentally [3–6], however, numerical investigations have been performed by modelling single microdischarges only (e.g. [1, 7–16]), where the multichannel structure and channel interaction via surface charges are not taken into account.

2. Numerical model

A two-dimensional model for description of a single microdischarge has been presented in [1]. For a discharge in a CD arrangement with extended electrodes (e.g. long thin stripes embedded in a dielectric plate), however, one has to consider a multitude of discharge channels distributed on the dielectric surface along the length of the electrode,

 © 2004 IOP Publishing Ltd Printed in the UK

which determine the behaviour of the device. That is, the characteristic parameters of such a device result from the sum of individual discharge channels. However, the appearance of channels is not independent of that of others. It is influenced by surface charges resulting from preceding channels, which change their distribution on the surface and influence local breakdown conditions.

To obtain realistic parameters of a CD device, the inter-channel distance and the channel width have been included in the model. With the help of these values the surface charge density of isolated channels has been averaged along the length of the electrodes. The new averaged charge density distribution together with the rising voltage determines the breakdown conditions for the next discharge pulse and so on. The average distance between adjacent channels of the discharge, which happen (nearly) simultaneously, is of the order of the inter-electrode distance [3, 4].

With the improved model some parameters of the device like capacitances and voltage–charge dependences have been obtained per unit length of electrode. These quantities can be compared with the experimental values of a real CD device if the actual configuration of the electrode system (distances between electrodes and between pairs of electrodes) is taken into account.

The device under consideration (basic configuration) is characterized by the following measures (if not otherwise mentioned):

(a) thickness of dielectric plate 1 mm,
(b) thickness of dielectric layer above electrodes 55 μm,
(c) thickness of electrodes 5 μm,
(d) width of electrodes 120 μm,
(e) gap between electrodes 80 μm,
(f) gap between pairs of electrodes 240 μm,
(g) relative permittivity 10,
(h) oxygen of 1.7 bar pressure.

3. Discharge development on pre-charged surfaces

First discharge pulses appear when the breakdown condition is reached along the pairs of electrodes. They charge the surface and change the initial field distribution (figure 2). If the voltage rises further on or changes its polarity, breakdown conditions can be reached again. The field distributions at breakdown for charged and uncharged surfaces are comparable (figures 2 and 3). In figure 3 a kind of shoulder can be detected. The shoulders result from surface charges left from previous discharge activities.

The discharge dynamics on pre-charged surfaces do not differ considerably from those on uncharged surfaces. A cathode-directed streamer appears between the electrodes and moves to the position of the far edge of the cathode, and a cathode layer develops. A weak anode-directed streamer moves along the anode and a well conducting region appears between the electrodes (electron phase). The space charge resulting from the streamers together with the charges collected on the surface gives a dipole, which reduces the external field. During the following ion phase the space charge disappears.

The surface charge distribution depends on whether the voltage polarity of the succeeding discharge pulse is

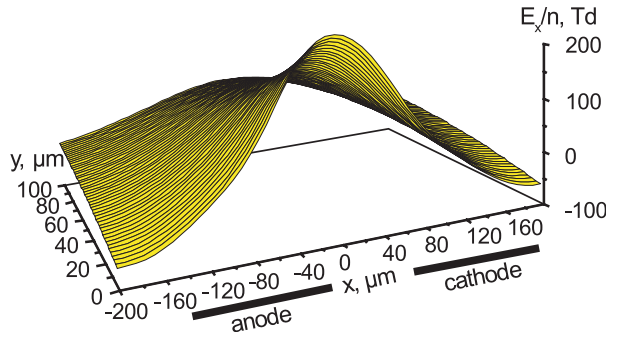

Figure 2. Tangential electric field strength component above the uncharged dielectric surface (2100 V, 1.7 bar oxygen, basic configuration).

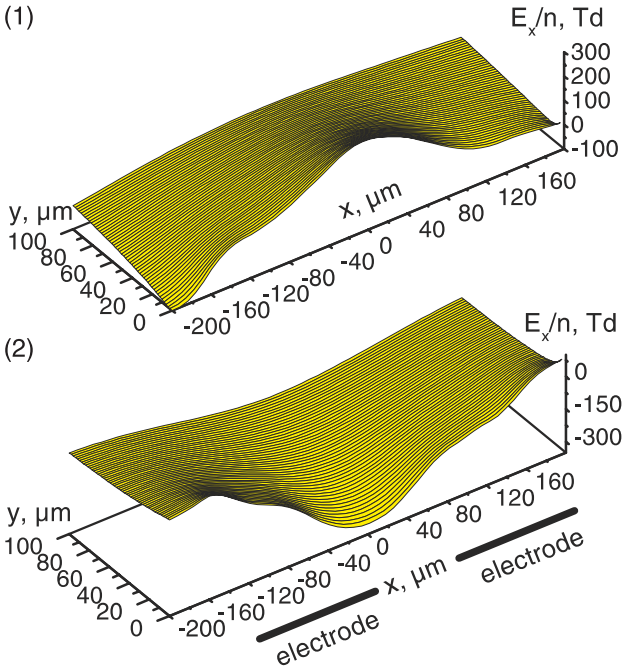

Figure 3. Tangential electric field strength component on a pre-charged surface for positive (1) and negative (2) polarity at breakdown condition (basic configuration).

changed or not. With the same polarity the surface charge density increases, and while applying the opposite polarity it decreases.

The current pulses belonging to pre-charged surfaces have nearly the same shape as those with uncharged ones; however, a small extension of the current duration occurs. The amplitude of the current pulse is independent of the initial conditions. Its absolute value is about 0.5 A per cm of electrode length. Approximately the same amount of charge is transferred in each current pulse. The surface charge density changes its sign periodically during the cycles of applied voltage (figure 4). The surface charge distribution is always bipolar. The width of the charged regions depends on time. After a half cycle of the applied voltage the charge density distribution is always comparable, though, with opposite polarity. The maximum charge density is about 200 nC cm^{-2} at a voltage amplitude of 3.5 kV (figure 4).

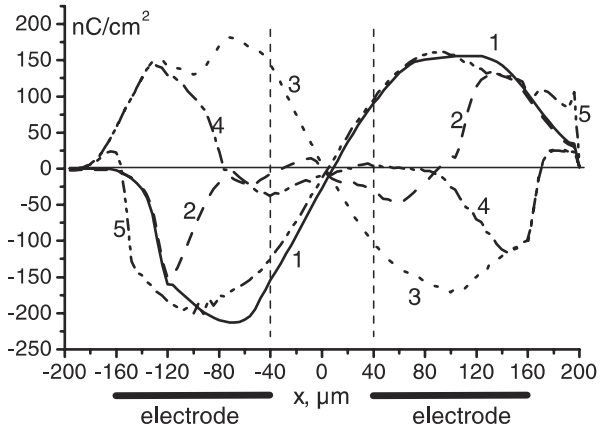

Figure 4. Distribution of the surface charge density during a cycle of the applied voltage (the numbers from 1 to 5 denote consecutive current pulses).

4. Variation of the dimensions of the electrode system

From modelling results it follows that the discharge dynamics does not change remarkably if the dimensions of the electrode system are changed. However, some device properties change: the initial field strength distribution, the shape of the current pulse, the ignition voltage and the capacitance of the device.

In order to find out these changes the thickness of the dielectric layer (Δ) and the electrode gap (d) have been varied from 25 μm to 200 μm and 80 μm to 480 μm, respectively. The value of the relative dielectric constant was changed from 5 to 15.

4.1. Initial electric field strength distribution

The maximum of the tangential component of the field strength is first in the middle of the electrode gap as long as the gap is small (figure 5). On increasing the thickness of the dielectric layer the distribution becomes wider and smoother. If the electrode distance is increased further, the field distribution becomes more flat. With large electrode gaps and a small dielectric layer, two maxima of the tangential component of the field strength appear at the edges of the electrode position (figure 5). The field strength distribution becomes more similar to that of isolated electrodes.

Independent of the electrode arrangement, the discharge dynamics are comparable. Two peaks of field strength appear between the electrodes and propagate along the surface, directed against one another. The cathode-directed streamer is more pronounced, its head moving about 10–20 μm above the dielectric surface. It reaches the dielectric surface with a field strength value close to that of the normal cathode fall. The velocities of the two streamers are nearly identical. In between the streamers the normal component of the field strength becomes zero due to charge accumulation on the dielectric surface.

The value of the field strength enhancement in the streamer heads depends (apart from polarity) on the thickness of the dielectric layer. With increasing thickness the two enhancements become closer in value and the size of the discharge region increases due to the increased width of

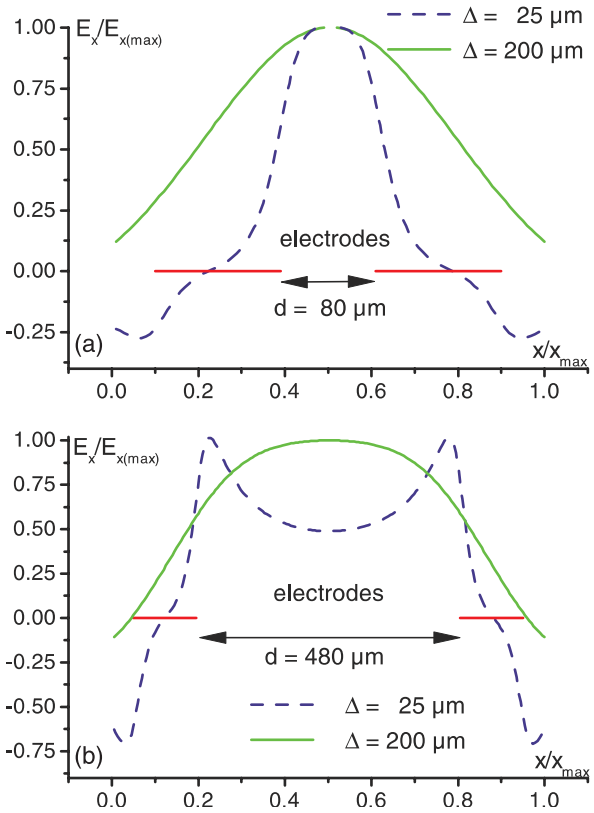

Figure 5. Normalized tangential component of the initial field strength (related to its maximum value) at a thickness of the dielectric layer above the electrodes of 25 and 200 μm for an electrode gap of (*a*) 80 μm and (*b*) 480 μm.

the field distribution (figure 5). On increasing the thickness of the dielectric layer from 25 to 200 μm the extension of the discharged area changes from 160 to 340 μm with the size of the electrode system remaining the same (inter-electrode distance 80 μm and electrode width 120 μm).

4.2. Shape of the current pulse

The electrode arrangement hardly affects the shape of the current pulse. The pulse duration is nearly constant. Only a small increase in the current duration has been found between the shortest and largest electrode distance.

The value of the relative permittivity is much more important for the current shape. On increasing its value from 5 to 15, the pulse duration nearly doubles (figure 6). The surface charge density increases in this case too.

A pressure increase accelerates the discharge process during cathode layer formation proportional to the pressure (current rise in figure 6), except for the lowest permittivity. In this case the total duration of the discharge process is extremely short. The total duration of the charge transfer decreases with increasing pressure (the durations of the current pulses at 1.0 and 2.4 bar for $\varepsilon = 10$ are 4 and 6 bar ns, respectively, i.e. 4 and 2.4 ns).

4.3. Ignition voltage and device capacitances

The value of the calculated ignition voltage increases with electrode distance and the thickness of the dielectric (table 1).

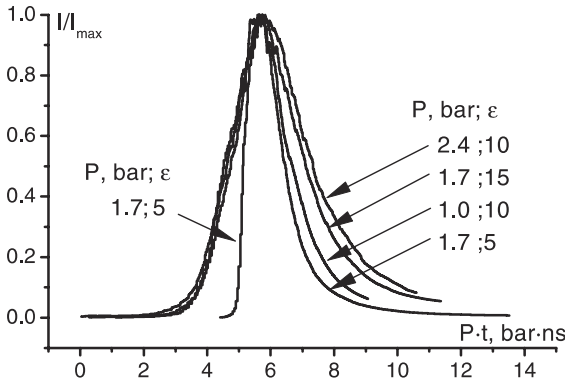

Figure 6. Related current shapes of discharge pulses for different values of oxygen pressure and permittivity.

Table 1. Influence of dielectric thickness (Δ) on ignition voltage in volts for different electrode gaps (d), gas pressure 1.7 bar.

d (μm)	$\Delta = 25\,\mu$m	$\Delta = 55\,\mu$m	$\Delta = 95\,\mu$m	$\Delta = 200\,\mu$m
80	1300	1900	2700	6500
480	4200	4800	5000	7000

Table 2. Capacitance of a CD device with an area of 0.04 m^2 (oxygen pressure 1.7 bar).

ε	5	10	15	Exp.
C_{eff} 'off', nF	4.5	10.7	14.2	9.7
C_{eff} 'on', nF	7.3	16.6	22.2	13.9

These dependences are non-linear. Increasing the electrode gap six times from 80 to 480 μm, the breakdown voltage rises only 2.5 times. On increasing the thickness of the dielectric eight-fold from 25 to 200 μm, the ignition voltage increases less than two times (table 1, $d = 480\,\mu$m).

A variation of the dimensions of the electrode system not only changes the ignition voltage but the effective capacitance of the system as well (see section 5.1). One has to distinguish between a capacitance with discharge (discharge 'on') and without (discharge 'off'). Both capacitances decrease with a growing electrode gap. Increasing the electrode gap six-fold, the capacitances decrease about two times (table 2).

An increase in the dielectric thickness results in an increase in the capacitance. An increase in the dielectric layer above the electrodes denotes a larger part of the system consists of the dielectric with a higher value of the relative permittivity.

Even by changing the dimensions, the general behaviour of the CD arrangement as well as some discharge parameters (charge and neutral particle distributions, surface charge density, process efficiency, etc) are hardly influenced.

5. Features of extended electrode systems

5.1. Lissajous figure

In order to be able to compare modelling with experimental results, charge–voltage diagrams (Lissajous figures) have been simulated. In general the Lissajous figure of dielectric barrier discharges (DBDs) is a parallelogram, which consists of straight lines with two different slopes (figure 7). The lines

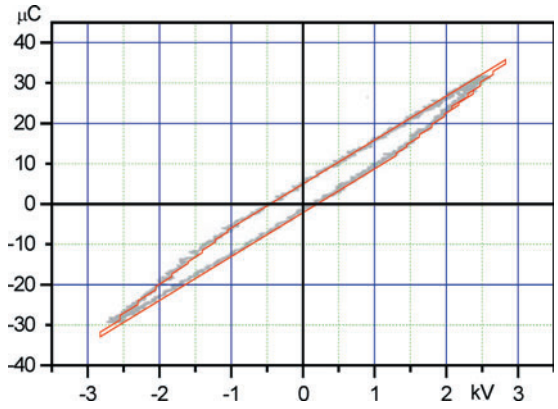

Figure 7. Experimental (grey) and simulated (red, black in the printed journal) Lissajous figures (1.7 bar oxygen, discharge area 0.04 m^2).

Table 3. Inception voltage at different relative permittivities (parameters as in figure 7).

ε_{r}	5	10	15	Experiment (10/11.5)
Inception voltage (kV)	2.4	1.9	1.8	1.9

with smaller gradient belong to the displacement charge (no discharge in the gas space on the surface of the device), while the steeper gradients begin at a voltage level that is equal to the discharge inception voltage (of the system) and belong to the displacement current plus the current of the transferred charge in the gas space. This part of the Lissajous figure consists in principle of many tiny steps (charge jumps) resulting from different discharge channels. Averaging these steps by linear approximation, one obtains the lines of the Lissajous figure with the larger gradient.

The simulation results presented in figure 7 belong to a CD device with an electrode distance of 80 μm, an electrode width of 120 μm and a total discharge area of 0.04 m^2 with an electrode length of about 80 m. In figure 7 the corresponding experimental curve is presented as well. The agreement is quite satisfactory.

From the Lissajous figure one can conclude that the discharge device behaves like a capacitive element of the circuit with a change in capacity during discharge operation. As already mentioned before, the discharge increases the capacitance of the device. Two capacitances can be derived from the figure, the capacitance of the device without discharge burning (discharge 'off') and with discharge already ignited (discharge 'on').

The inception voltage of the device is influenced by the permittivity of the dielectric (table 3). The experimental and simulated values of the inception voltage are in accordance. This is especially true for the relative permittivity 10, which is close to that of the experimental device.

The accuracy of the simulation results depends on the dimension of the electrode system, which is better for compact arrangements. The maximum deviation from experimental data of about 20–25% was found for an electrode system with a width of about 0.6–0.7 mm. In general, some adjustments of the model parameters, such as swarm parameters and rate constants, may improve the results.

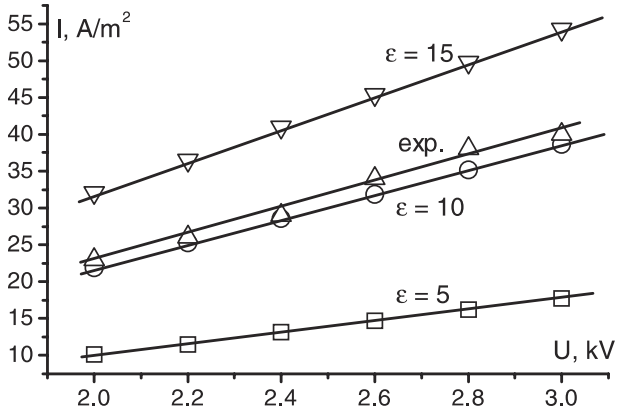

Figure 8. Current density on the electrode area for different values of the dielectric constant (10 kHz, 1.7 bar oxygen).

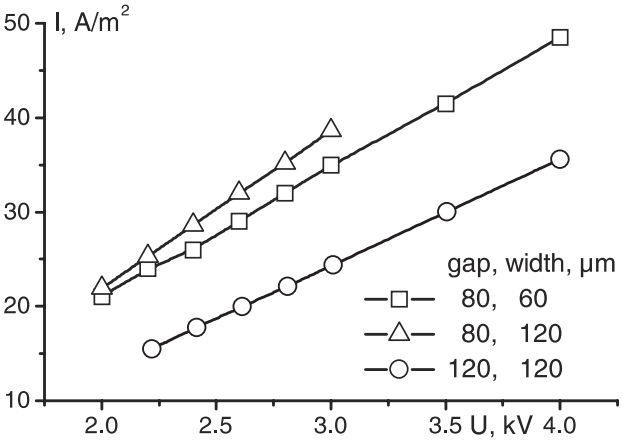

Figure 9. Specific current density on the electrode area for different electrode systems (inter-electrode distance and width of the electrodes; 1.7 bar oxygen, 10 kHz).

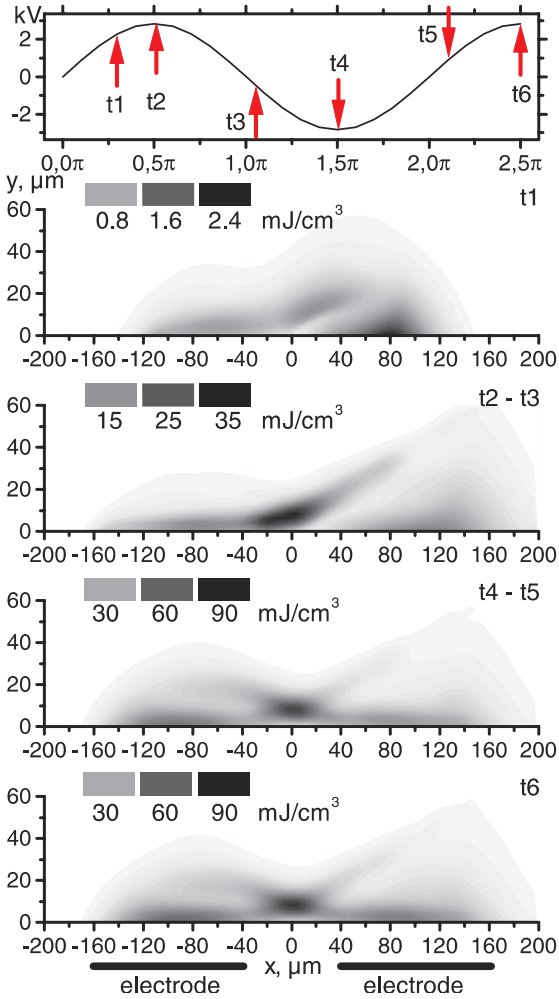

Figure 10. Distributions of the energy density in the gas region above the dielectric surface at different phases, t1–t5, of the applied voltage (voltage amplitude 2.9 kV, oxygen pressure 1.7 bar).

5.2. Current density

The current of the CD device (displacement plus transferred) depends on the voltage amplitude, frequency and size of the electrode system and that of the whole device. Experimental and simulated results were compared for a frequency of 10 kHz.

The current density of the discharge area is proportional to the applied voltage and nearly linear proportional to the permittivity (figure 8). The experimental results for a relative permittivity of about 10 are in rather good correspondence with the simulated ones. The current densities for other frequencies can be derived from figure 8 by multiplying the data with the frequency ratio.

An enlargement of the inter-electrode distance increases the breakdown voltage. On the other hand the length of the electrode system per area unit rises with decreasing electrode gap. The final result is that the current density declines with increasing size of the electrode system (figure 9). For example the length of the electrode system per area unit, for a system with an electrode width of 120 μm, is about 20% shorter compared with an electrode width of 60 μm and the same electrode gap. Nevertheless, the current density is 10% larger. This means that wider electrodes induce an about 30% larger current density per unit of the electrode length. The variation can be explained by differences in the discharge dynamics, which depends on the width of the electrode. On broader electrodes the discharge spreads over a larger area of the electrodes and more charge is collected on the surface.

5.3. Energy density and yield of oxygen dissociation

The energy consumption of a DBD device and its efficiency of, e.g. oxygen dissociation is determined by the properties of single discharge channels (compare figures 11 and 12 of [1]). The energy release in the discharge area above the dielectric surface of a CD device happens with current pulses (figure 10). The energy density distribution is unsymmetrical. There are two maxima belonging to the movement of electrons and ions near the anode and cathode, respectively. After the first current pulse the maximum energy density is about 2 mJ cm^{-3} (figure 10).

If the voltage amplitude is high enough, several discharge pulses (sets of discharge channels) happen during the voltage rise. The distribution of the energy density changes: it becomes more symmetric and smooth. At opposite polarity (t3 in figure 10) a further charge transfer happens up to the voltage peak (t4 in figure 10), increasing the energy density further. With an ac supply the next discharge pulse appears at t5 and

so on. In general the value of the voltage at t5 differs from that at t1. The difference is caused by the charge, which is accumulated on the surface during the preceding discharge pulses.

After a cycle of the applied voltage the energy density is nearly symmetrically distributed, with a main maximum in the centre of the discharge region (figure 10). Above the electrodes two additional maxima of energy density appear: these can be attributed to the cathode region at each half period of the applied voltage.

In investigations of oxygen dissociation (ozone production), a frequency of up to 10 kHz has been considered. That is, a period of the applied voltage lasts a minimum of 100 μs. The characteristic time of heat transfer (from the gas space through the dielectric bulk to a cooling system on the reverse of the dielectric) is of the same order of magnitude. Following from this, heat transfer must be included in a model if more than a period is simulated. In general, the heat transfer shifts the energy density distribution to the dielectric surface and limits its maximum value.

As shown in [1], the discharge process is less intensive in the Q = const case. The value of the transferred charge is about half of that in the V = const case, and the energy consumption is about 25% smaller (table 1 of [1]). However, the efficiency of oxygen atom production or ozone synthesis is practically the same (5% lower in table 1 of [1], but this difference is within the scatter of the modelling results).

Ozone synthesis starts a few microseconds later than the energy release. The distribution of the ozone concentration is shifted towards the anode after the first discharge pulse (figure 11). The maximum ozone concentration is found in the midst of the discharge region after several discharge pulses and, especially, after polarity change (figure 11).

The distribution of the ozone density reveals additional information about the structure of the energy density distribution. There are three maxima of energy density; however, there is only one of the ozone concentration (compare figure 10 with figure 11). There is no significant amount of ozone in the cathode regions of the two half cycles. The electron density is too low to generate a significant number of radicals, while the mean energy of ions is not high enough to dissociate molecular oxygen.

6. Discussion

Plasma-chemical reactors with CD arrangements are used to treat gases, e.g. to generate radiation in plasma display panels and dissociate oxygen for ozone production. The constructional parameters of the arrangement (inter-electrode distance, thickness of the dielectric layer, its relative permittivity, etc) affect the operating parameters of the reactor, although, looking at ozone synthesis, the efficiency of the reactor remains nearly constant (table 4). The scatter is less than 15%. With respect to the accuracy of the rather sophisticated simulations, the results are therefore not far from being equal and are in good agreement with experiments [5]. Moreover, these values are practically identical to the efficiency values of other DBD arrangements, e.g. with a gas gap.

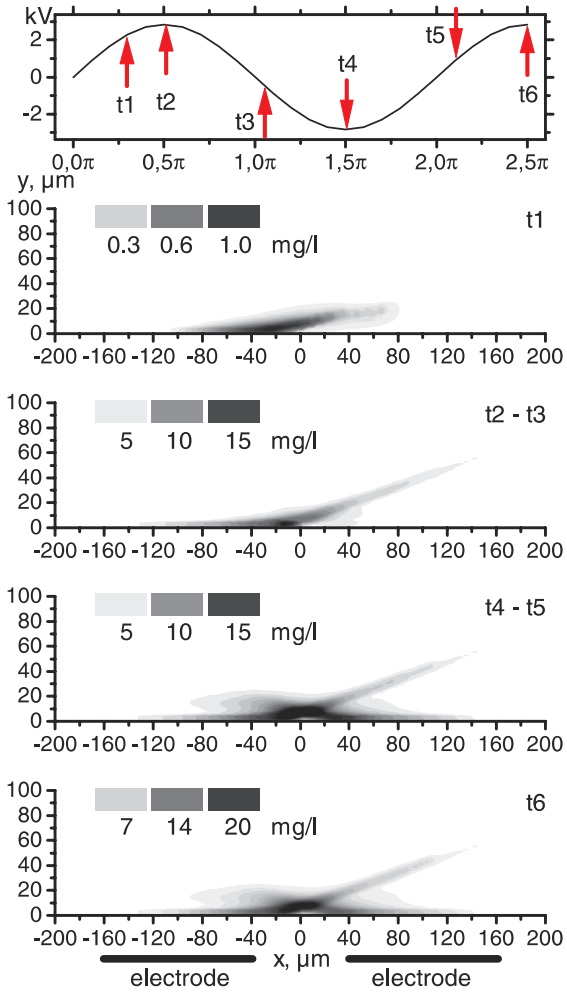

Figure 11. Distributions of the ozone concentration in the gas region above the dielectric surface at different phases, t1–t5, of the applied voltage (voltage amplitude 2.9 kV, oxygen pressure 1.7 bar).

Table 4. Energy consumption of ozone synthesis for different conditions.

Constructional parameters (μm) (electrode width, electr. distance)	Relative permittivity	Pressure (bar)	Energy consumption (kWh kg^{-1}(O_3))
(120, 80)	5	1.7	7.6
(120, 80)	15	1.7	6.7
(60, 80)	10	1.7	6.8
(120, 120)	10	1.7	6.5
(120, 80)	10	1.0	6.9
(120, 80)	10	2.4	7.2
Experimental value [5]		1.7	6.3

Comparing the maximum efficiency of different types of optimized DBD ozone generators, one realizes that it is nearly identical. Subsequently the conditions for ozone synthesis must be identical as well. The most energetic phase of DBDs is the electron phase, starting with the development of the streamer. The maximum values of the field strength occur in the streamer head and the cathode fall. In the streamer head the electron density and the field strength are high enough for efficient oxygen dissociation. The maximum efficiency occurs here; however, the spatial–temporal volume of the

streamer head is rather small to be able to produce a remarkable amount of ozone. In the cathode layer the highest field strength is found; however, the electron density is rather low here to contribute to ozone synthesis. The main source of ozone is the conductive channel of the discharge between the positions of the electrodes. The field strength in the channel is about 70–100 Td. This value is high enough for a significant dissociation rate. The synthesis efficiency (at 100 Td) is about half the maximum value experimentally found, about 140–160 g O_3 kWh^{-1} (figure 14 of [1] and table 4). This value is reached in ozone generators (from oxygen) with quite different DBD arrangements.

In any DBD arrangement the formation of a conductive region (channel) behind the cathode-directed streamer and its properties are nearly identical. The mean field strength in this region is an equilibrium value, at which electron multiplication and convection is balanced by attachment processes. The field strength value is a characteristic for the applied type of gas but does not depend on the DBD arrangement.

In oxygen the equilibrium value is close to 100 Td; in electropositive gases, like noble gases, it is only a few Townsends. A few Townsends is not sufficient to produce excited particles and radicals effectively. In this case the streamer head may be the main source of excited particles and radicals.

7. Conclusions

A modified self-consistent two-dimensional model of CD has been developed. Basically it is a two-dimensional model, in which some three-dimensional parameters of the CD are inserted, namely the thickness of discharge channels and the mean inter-channel distance. Unlike common physical and mathematical approaches, the model is characterized by the following:

(i) Photo-emission on surfaces is taken into account.
(ii) Special care is taken regarding the field definition at the dielectric boundary.
(iii) The numerical procedure used allows a precise description of rapid and small-sized phenomena like streamer or ionization waves (explicit method).

Using this model the influence of the thickness of the dielectric layer covering the electrodes, the value of the dielectric constant, the pressure and the dimensions of the electrode system on the discharge properties and dynamics are investigated apart from the properties of CD devices as a whole.

The ignition voltage of a CD device is slightly decreasing with rising value of the dielectric constant and depends on the dimensions of the electrode system.

The surface charge, which is left by preceding discharge activity, is taken into account by simulating the discharge dynamics. Surface charges modify the field strength distribution to some extent, while the breakdown process and the overall discharge dynamics are qualitatively unchanged. The surface charge distribution changes its value and sign during a period of the applied voltage.

The current shape (amplitude and duration) is hardly influenced by the discharge conditions, e.g. by the gas pressure and dimensions. The effective capacitances of the CD device (capacitance discharge 'on' and 'off') depend on the dimensions. The simulated values are in good agreement with experimental ones.

The simulated Lissajous figure coincides practically with the corresponding experimental one. That is why the value of the specific current density (per unit area of discharge surface) of a real CD device, which is derived from a Lissajous figure, corresponds with measured values rather well. Its value increases with the permittivity of the dielectric and the width of the electrodes; however, it decreases with pressure and electrode distance.

It is necessary to note that the efficiency of electric energy transformation to internal molecular states (for instance, dissociation of molecular oxygen or, in other words, ozone synthesis) is hardly affected by the parameters mentioned above. This phenomenon exists because the main energy release happens in the high conduction channels, whose parameters depend on the properties of the fed gas only. Although the discharge conditions such as pressure, permittivity and dimensions of the electrode system affect the dynamics of the appearance and development of discharge channels and their size, the internal conditions remain practically unchanged.

Acknowledgments

The investigations were carried out mainly in the frame of a cooperation with Toshiba Corp., Japan. The authors wish to express thanks to Dr Takaii Murata and his colleagues for their contribution. Part of the investigations have been supported by the International Bureau of the Federal Ministry of Education and Research of Germany in the frame of bilateral co-operation in science and technology.

References

[1] Gibalov V I, Murata T and Pietsch G J 2004 Dynamics of dielectric barrier discharges in coplanar arrangements *J. Phys. D: Appl. Phys.* **37** 2082–92
[2] Müller I, Punset C, Ammelt E, Purwins H-G and Boeuf J P 1999 Self-organized filaments in dielectric barrier glow *IEEE Trans. Plasma Sci.* **27** 20–1
[3] Hulka L and Pietsch G J 2002 On the ignition voltage and structure of coplanar barrier discharges *Contrib. Papers Int. Symp. on High Pressure, Low Temp. Plasma Chemistry (HAKONE VIII) (Pühajärve, Estonia)* vol II, pp 259–63
[4] Murata T, Okita Y and Terai K 1997 Distribution of surface discharge for ozone generation *Proc. 23rd Int. Conf. on Phenom. in Ionized Gases (Toulouse)* vol III, pp 82–3
[5] Murata T, Okita Y, Noguchi M and Takase I 2001 Basic parameters of coplanar discharge ozonizer *Proc. 15th World Congress of the Int. Ozone Association (London)* vol III, pp 39–54
[6] Okita Y, Iijima T, Amano A, Yamanashi I and Murata T 2003 Development of compact 1 kg h^{-1} coplanar discharge ozonizer *IEEJ Trans. FM (Fundamentals and Materials)* **123** 39–54 (in Japanese)
[7] Gibalov V I, Murata T and Pietsch G J 2000 Modelling of the discharge development in coplanar arrangements *Proc. 13th Int. Conf. on Gas Discharges and their Applications (Glasgow)* vol I, pp 275–8
[8] Gibalov V I, Murata T and Pietsch G J 2002 Parameters of barrier discharges in coplanar arrangements *Contrib. Papers*

Int. Symp. on High Pressure, Low Temp. Plasma Chemistry (HAKONE VIII) (Pühajärve, Estonia) vol I, pp 152–7

[9] Gibalov V I, Murata T and Pietsch G J 2002 Some characteristic parameters of coplanar discharge arrangements *Proc. 14th Int. Conf. on Gas Discharges and their Applications (Liverpool)* vol I, pp 183–6

[10] Rauf S and Kushner M 1999 Dynamics of coplanar-electrode plasma display panel cell I. Basic operation *J. Appl. Phys.* **85** 3460–9

[11] Rauf S and Kushner M 1999 Dynamics of coplanar-electrode plasma display panel cell II. Cell optimization *J. Appl. Phys.* **85** 3470–6

[12] Boeuf J P, Punset C, Hirech A and Doyeux H 1997 Physics and modeling of plasma display panels *J. Phys. IV* **C4** 3–14

[13] Cambell R B, Veerasingam R and McGrath R T 1995 A two-dimensional multispecies fluid model of plasma in an AC plasma display panel *IEEE Trans. Plasma Sci.* **23** 698–708

[14] Punset C, Boeuf J P and Pitchford L C 1998 Two-dimensional simulation of an alternating current matrix plasma display cell: cross-talk and other geometric effects *J. Appl. Phys.* **83** 1884–97

[15] Shin Y K, Lee J K and Shon C H 1999 Two-dimensional breakdown characteristics of PDP cells for varying geometry *IEEE Trans. Plasma Sci.* **27** 14–5

[16] Jeong H S, Shin B-J and Whang K-W 1999 Two-dimensional multifluid modeling of He-Xe discharge in an AC plasma display panel *IEEE Trans. Plasma Sci.* **27** 171–81